



# Kinetic model of chromium release from argon oxygen decarburisation (AOD) slag in a neutral leachate

Ya-nan Zeng<sup>1</sup> · Qian-qian Ren<sup>1</sup> · Bao Liu<sup>1</sup> · Jun-guo Li<sup>1</sup>

Received: 9 October 2019 / Revised: 26 February 2020 / Accepted: 26 February 2020 / Published online: 9 June 2020  
© China Iron and Steel Research Institute Group 2020

## Abstract

Valorisation of argon oxygen decarburisation (AOD) slag, a suitable recycling resource, is limited by the release of a notable amount of heavy metals, such as chromium. The mineralogical component of AOD slag was characterised by X-ray diffraction and scanning electron microscopy-energy-dispersive X-ray spectrometry. To explore the release kinetics of chromium from AOD slag, neutral leaching tests were performed at various temperatures. The results indicated the existence of two leaching stages: quick and slow leaching stages. In 2 h, the chromium release fraction increased sharply as the leaching time increased. As the leaching time increased, the chromium release rate gradually decreased. Based on the shrinking core model, chromium release kinetic models for the quick and slow leaching stages from the AOD slag were independently determined. The chromium release was controlled by solid product diffusion during the quick leaching stage and a complicated process in the slow leaching stage. The activation energy of chromium leaching was calculated based on the Arrhenius equation. Solid product diffusion was the velocity-determining step during the 2 h leaching process. In the slow leaching stage, chromium release was controlled by complicated hybrid control dominated by solid product diffusion.

**Keywords** Kinetic model · Chromium release · Shrinking core model · AOD slag

## 1 Introduction

Argon oxygen decarburisation (AOD) slag, which is a type of by-product produced in stainless steel refining processes, can be used as supplementary material in the production of clinker, cement, concrete and other construction materials [1–5]. Approximately 1.8 million tons of AOD slag, which contains 9540 tons of chromium, are generated annually in China [6]. The potential release of chromium from AOD slag causes environmental concern. The leaching risk from AOD slag also severely limits its valorisation in the comprehensive utilisation of AOD slag. Therefore, the leaching toxicity and transformation mechanism of chromium in AOD slag need to be explored to improve the management and valorisation of AOD slag.

In general, chromium is present as trivalent chromium and hexavalent chromium due to rainwater leaching. Trivalent chromium is nearly harmless to the environment due to its

low mobility and toxicity. However, hexavalent chromium, which is a toxic substance due to its high oxidation capacity, is readily transported and accumulated in plants, which poses a serious health threat to mankind through the food chain. Chromium released from AOD slag is significantly impacted by the mineralogical components of AOD slag and the electrochemical characteristics of leachates [7–10]. Some leaching tests have been performed using toxicity characteristic leaching procedure (TCLP) and GB 5086.2-1997 to measure the leaching concentration of chromium [11]. The results indicated that the released chromium consists of trivalent chromium with leaching concentrations of 0.01–0.05 mg/L, which presents a minor eco-risk. However, in another study, the leached chromium consisted of hexavalent chromium with a concentration of 3 mg/L when the pH of the leachates was maintained at 8.0 [12]. The leaching concentration of chromium and its speciation are significantly influenced by the pH of the leachates. Moreover, the revised Pourbaix diagram for the Cr-H<sub>2</sub>O system reported by Beverskog illustrates the influence of redox potential (Eh) and pH on the chromium speciation in leachates [13].

With regard to the impact of the mineralogical component of the AOD slag, Kuhn and Mudersbach [14] related the

✉ Jun-guo Li  
lijg99@163.com

<sup>1</sup> School of Metallurgy and Energy, North China University of Science and Technology, Tangshan 063200, Hebei, China

chromium leaching concentration to the spinel phases. The increase in the content of spinel phases in the slags could effectively reduce the release concentration of chromium from the slag. Moreover, Samada et al. [12] synthesised a pseudobinary phase (e.g.  $\text{Ca}_2\text{SiO}_4\text{-MgCr}_2\text{O}_4$ ) to investigate the leaching law of chromium from chromium-bearing spinel phases. The results indicated that a solid solution of  $\text{MgCr}_2\text{O}_4$  in  $\text{Ca}_2\text{SiO}_4$  could enhance the leaching concentration of chromium from  $\text{MgCr}_2\text{O}_4$ . The type of chromium-bearing crystal phases might control the release behaviour of chromium into leachates.

Kinetic models of heavy metal release have been extensively investigated because these models are important for toxicity assessments of solid waste [15, 16]. However, few studies on the release kinetics of chromium from AOD slag have been reported. In this study, the release kinetics of chromium from AOD slag were explored based on the HJ557-2009 leaching method (solid waste-extraction procedure for leaching toxicity-horizontal vibration method, China). X-ray diffraction and scanning electron microscopy-energy-dispersive X-ray spectrometry (SEM-EDX) were employed to identify the mineralogical components of the AOD slag. The shrinking core model (SCM) was used to establish a kinetic model for chromium release from AOD slag. Moreover, the activation energy for chromium release from AOD slag during the quick and slow leaching stages was calculated based on the leaching data for chromium at different temperatures to evaluate the validity of the kinetic model.

## 2 Materials and methods

### 2.1 Materials

The AOD slag used in this work was obtained from a Chinese stainless steel factory. The sampled AOD slag was sieved through a 75- $\mu\text{m}$  sieve. The oversized material (~15 wt.%) contained large particles and several metal pieces that were discarded. The undersized material was used for mineralogical analysis and leaching tests after the slag was dried for 6 h at 105 °C to remove the moisture that was adsorbed during the air-cooling and water-spraying processes. The chemical composition of the AOD slag was analysed using the chemical analysis method YBT 140–1998 and is shown in Table 1. As shown in Table 1, this slag was rich in CaO with a content of 55.90 wt.%. The content of  $\text{SiO}_2$  was 24.67 wt.%. The third dominant oxide component was MgO with a content of 5.85 wt.%. Therefore, this slag was an alkaline waste with a ternary basicity ( $(w_{\text{CaO}} + w_{\text{MgO}})/w_{\text{SiO}_2}$ ) of 2.50. This AOD slag also

contained 1.07 wt.%  $\text{Al}_2\text{O}_3$ , 1.15 wt.% FeO, 0.16 wt.% MnO and 0.88 wt.%  $\text{TiO}_2$ . The chromium was enriched as  $\text{Cr}_2\text{O}_3$  with a content of 0.51 wt.%.

### 2.2 Mineralogical analysis

The mineralogical components of the AOD slag were determined by X-ray diffraction (XRD). The measurements were performed on a D/MAX2500PC automatic diffractometer with a continuous scanning device using Cu  $\text{K}\alpha$  radiation at 100 mA and 40 kV with a scanning velocity of 10 ( $^\circ$ )/min over a 10 $^\circ$ –90 $^\circ$  2 $\theta$  range. Figure 1 shows the XRD patterns of the AOD slag. As shown in Fig. 1, the main mineral phases in this slag were dicalcium silicate ( $\text{Ca}_2\text{SiO}_4$ ), merwinite ( $\text{Ca}_3\text{MgSi}_2\text{O}_8$ ), pyroxene ( $(\text{Ca,Mg,Al})_2(\text{Si,Al})_2\text{O}_6$ ) and periclase (MgO). Chromium-bearing minerals were not detected in the XRD patterns due to their trace contents.

To investigate the chromium-bearing phases, SEM with mapping by EDX was performed. The microstructure of the AOD slag is shown in Fig. 2. The existing elements and their contents in micro-area 1 in Fig. 2 are listed in Table 2.

The results in Fig. 2 indicate that the mineral phases in the AOD slag were present as heterogeneous grains. Partial mineral particles existed as clintheriform and massive aggregates, whose particle sizes were 10–70  $\mu\text{m}$  and 20–90  $\mu\text{m}$ , respectively. Although no pure chromium-bearing mineral phases were detected in the field of vision, a chromium-bearing multiphase was observed in micro-area 1. As listed in Table 2, Ca and Si were the two major elements in micro-area 1, and the mole ratio of Ca to Si was approximately 2.1. Therefore, micro-area 1 most likely contained

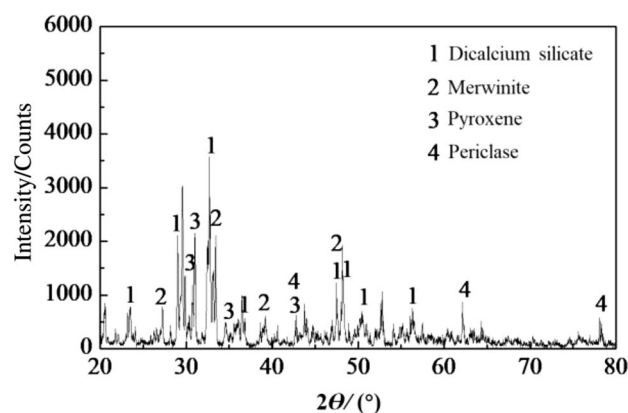
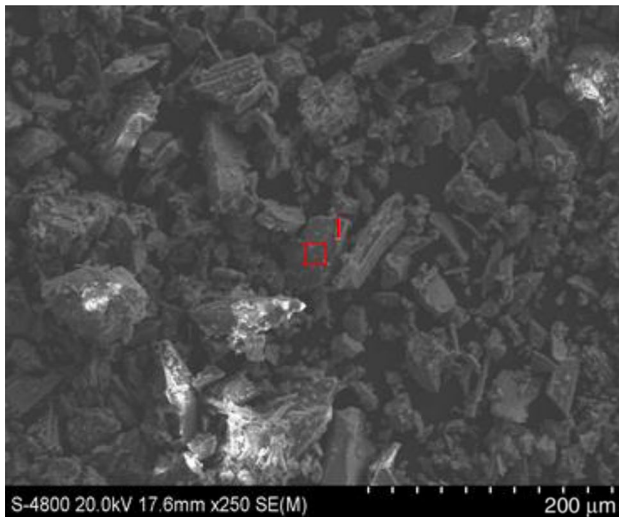


Fig. 1 X-ray diffraction patterns of AOD slag

Table 1 Chemical composition of AOD slag (wt.%)

CaO	$\text{SiO}_2$	MgO	$\text{Al}_2\text{O}_3$	$\text{Cr}_2\text{O}_3$	FeO	MnO	$\text{TiO}_2$	S	P	Others
55.90	24.67	5.85	1.07	0.51	1.15	0.16	0.88	0.069	0.014	9.73



**Fig. 2** Microstructure of AOD slag observed by SEM

**Table 2** Existing elements and their contents in micro-area 1 in Fig. 2 (wt.%)

O	Mg	Si	Ca	Cr
42.90	2.03	13.36	40.94	0.77

dicalcium silicate. As assumed by Samada et al. [12], a pseudobinary phase, such as  $\text{Ca}_2\text{SiO}_4\text{-MgCr}_2\text{O}_4$ , could exist in the AOD slag. The mole ratio of Mg to Cr in micro-area 1 was 5.67. Therefore, a certain amount of  $\text{MgCr}_2\text{O}_4$  along with MgO may have been simultaneously dissolved into  $\text{Ca}_2\text{SiO}_4$ , resulting in the formation of a chromium-bearing multiphase.

### 2.3 Leaching test

The leaching tests were performed using the HJ557-2009 leaching method to investigate the leaching kinetics of chromium from AOD slag and the influence of temperature on chromium release. Ultrapure water ( $18.2 \text{ M}\Omega/\text{cm}$ ) with a pH of 7.0 was used as a neutral leachate. Ten grams of AOD slag were rotated with 100 mL of ultrapure water at a speed of 30 r/min. Moreover, the leaching temperatures were selected to be 20, 30, 40, 50 and 60 °C. The leaching tests were performed under closed conditions to prevent any significant atmospheric additions of carbon dioxide or oxygen. 5 mL of leachate was sampled at different time. The sampled leachate was replaced with the same volume of ultrapure water to maintain a constant liquid-to-solid ratio. The sampled leachates were filtered through  $0.22 \mu\text{m}$  membrane filters, and the concentration of chromium in these leachates

was measured. The chromium content was determined using diphenylcarbazide spectrophotography (GB7467-87, 1995) associated with the oxidation of ammonium peroxydisulfate [17, 18].

## 3 Results and discussion

### 3.1 Chromium release fraction at different temperatures

According to the concentrations of chromium in the leachates, the mass of the chromium released from AOD slag at different time can be calculated. The released chromium mass divided by the total mass of chromium in the AOD slag was equivalent to the chromium release fraction at different leaching time. Figure 3 shows the influence of temperature on the chromium release fraction. As shown in Fig. 3, during the 12 h leaching period, two leaching stages existed: the quick leaching stage and the slow leaching stage. During the quick leaching stage (in 2 h), the chromium release fraction increased sharply as the leaching time increased regardless of the leaching temperature. The chromium release fraction increased slowly after 2 h; this stage was the slow leaching stage. As the temperature increased, the chromium release fraction increased significantly for the same leaching time. After 12 h of neutral leaching, the chromium release fractions at 303.15, 313.15, 323.15 and 333.15 K were 1.14, 1.52, 1.73 and 1.94 times higher than that at 293.15 K, respectively.

### 3.2 Kinetic model of SCM

The SCM is the most successful model for describing the leaching kinetics of heavy metals from solid waste [15, 16, 19]. In this kinetic model, three steps are considered to be

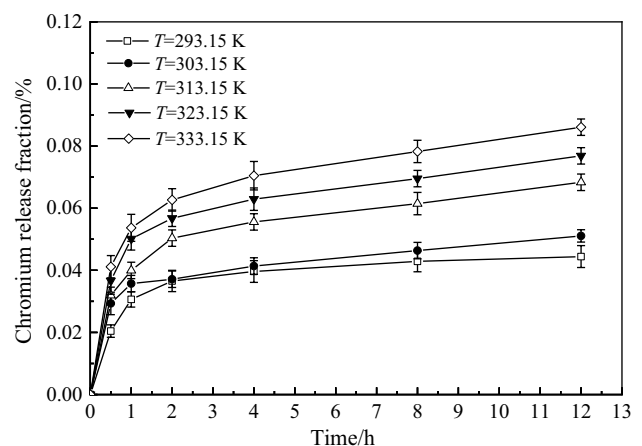


**Fig. 3** Influence of temperature  $T$  on chromium release fraction

controlling factors for the release of heavy metals, including liquid film diffusion control, solid product diffusion control and reaction control. During the neutral leaching of the AOD slag, the particle size of the original phase in the solid waste decreased gradually due to its dissolution as the leaching time increased. The SCM model provides a suitable kinetic model for chromium release from AOD slag.

### 3.2.1 Liquid film diffusion control

According to the SCM, when the leaching kinetics of the diffusion material are controlled by liquid film diffusion, the fraction of chromium release at any time can be predicted by Eq. (1) [20]:

$$\frac{t}{\tau} = 1 - (1 - x)^{2/3} \quad (1)$$

where  $x$  is the chromium release fraction;  $t$  is the leaching time; and  $\tau$  is the time for complete disappearance of the original particle, which can be predicted by Eq. (2):

$$\tau = \frac{\rho R_0^2}{2bDc} \quad (2)$$

where  $\rho$  is the density of the AOD slag;  $R_0$  is the radius of the unreacted particle (i.e. original particle);  $b$  is the stoichiometric coefficient of the reaction; and  $D$  and  $c$  are the molecular diffusion coefficient and the concentration of the diffusion material, respectively.

As shown in Fig. 3, the chromium release rate during the first 2 h was significantly different from that after 2 h. Therefore, the boundary condition of chromium leaching after 2 h is likely to be quite different from that prior to 2 h. Equations (1) and (2) can only be used for the quick leaching stage and are not suitable for the slow leaching stage. Based on the leaching experiment, the release kinetics of chromium during the slow leaching stage can be calculated with the following boundary conditions. The leaching time started at  $t=2$  h. The chromium release fraction at the initial time was the value at 2 h. Therefore, the chromium release fraction at any time during the slow leaching stage can be predicted by Eq. (3) [15]:

$$\frac{t - t_1}{\tau} = 1 - \left( \frac{1 - x}{1 - x_1} \right)^{2/3} \quad (3)$$

where  $t_1=2$  h;  $x_1$  is the chromium release fraction at 2 h; and  $\tau$  can be predicted using Eq. (4):

$$\tau = \frac{\rho R_0^2 (1 - x_1)^{2/3}}{2bDc} \quad (4)$$

### 3.2.2 Solid product diffusion control

When the leaching kinetics of the diffusion material are controlled by solid product diffusion, the fraction of chromium release at any time can be predicted by Eq. (5) [20]:

$$\frac{t}{\tau} = 1 - 3(1 - x)^{2/3} + 2(1 - x) \quad (5)$$

As previously mentioned, Eq. (5) cannot be fitted to the slow leaching stage due to the variation in the boundary conditions. The alternative equations are as follows [15]:

$$\frac{t - t_1}{\tau} = 1 - 3 \left( \frac{1 - x}{1 - x_1} \right)^{2/3} + \left( 21 - (1 - x_1)^{1/3} (x - x_1) \right) \quad (6)$$

$$\tau = \frac{\rho R_0^2 (1 - x_1)^{2/3}}{6bDc} \quad (7)$$

### 3.2.3 Reaction control

When the leaching kinetics of the diffusion material are controlled by the reaction between the original phase and the leachate, the chromium release fraction at any time can be predicted by Eq. (8) [20]:

$$\frac{t}{\tau} = 1 - (1 - x)^{1/3} \quad (8)$$

where  $\tau$  can be calculated using Eq. (9).

$$\tau = \frac{\rho R_0}{bk} \quad (9)$$

where  $k$  is the rate constant of the reaction. As previously mentioned, the kinetic equations during the slow leaching stage were converted into the following equations [15]:

$$\frac{t - t_1}{\tau} = 1 - \left( \frac{1 - x}{1 - x_1} \right)^{1/3} \quad (10)$$

$$\tau = \frac{\rho R_0 (1 - x_1)^{1/3}}{bk} \quad (11)$$

## 3.3 Kinetic model of chromium leaching from AOD slag

According to the leaching kinetic data shown in Fig. 3, chromium release from the AOD slag occurred in two stages (i.e. the quick and slow leaching stages). Due to the considered difference in the chromium release rates, the kinetic models for chromium release during the two

leaching stages were established separately. During the quick leaching stage, when the leaching kinetics of the diffusion material are controlled by liquid film diffusion, solid product diffusion and the reaction,  $1 - (1 - x)^{2/3}$ ,  $1 - 3(1 - x)^{2/3} + 2(1 - x)$ , and  $1 - (1 - x)^{1/3}$  should be in direct proportion to the leaching time  $t$  according to Eqs. (1), (5), and (8), respectively. During the slow leaching stage,  $1 - ((1 - x)/(1 - x_1))^{2/3}$ ,  $1 - 3((1 - x)/(1 - x_1))^{2/3} + 2(1 - (1 - x_1)^{1/3}(x - x_1))$ , and  $1 - ((1 - x)/(1 - x_1))^{1/3}$  should be in direct proportion to the leaching time  $(t - t_1)$ , respectively, according to Eqs. (3), (6), and (10).

### 3.3.1 Kinetic model during quick leaching stage

Based on the chromium release fraction in 2 h shown in Fig. 3, Eqs. (1), (5) and (8) are plotted as a function of time for the quick leaching stage in Fig. 4. In comparison with the correlation coefficients ( $R^2$ ) in Fig. 4a and c, the correlation coefficients shown in Fig. 4b were higher. This result indicates that chromium release from the AOD slag was controlled by solid product diffusion during the quick leaching stage.

As previously mentioned, chromium was dissolved in  $\text{Ca}_2\text{SiO}_4\text{-MgCr}_2\text{O}_4$ , which is a type of multivariate phase [12].  $\text{Ca}_2\text{SiO}_4$ , which is the major component in this multivariate phase, is freely soluble. During the quick leaching stage,  $\text{MgCr}_2\text{O}_4$  in the solid solution could easily come into contact with the leachate, and then, the reaction of chromium release occurred in a short period of time. The newly formed layer from the precipitation of the secondary phases during the 2 h leaching process, which consisted of okenite ( $\text{CaSiO}_3$ ), partlandite ( $\text{Ca}(\text{OH})_2$ ), brucite ( $\text{Mg}(\text{OH})_2$ ) and C-H-S gel ( $\text{CaH}_2\text{SiO}_4$ ), was thin. Therefore, the release rate of chromium was quick because it was easy for chromium to diffuse through the initial solid product layer. Moreover, the release rate of chromium was enhanced as the leaching temperature increased.

### 3.3.2 Kinetic model for slow leaching stage

Based on the chromium release fraction after 2 h, Eqs. (3), (6) and (10) are plotted as a function of time for the slow leaching stage in Fig. 5. In comparison with the correlation coefficients in Fig. 5a and c, the correlation coefficients shown in Fig. 5b were slightly higher. Solid product control is most likely type of kinetic control during the slow leaching stage. As the leaching time increased, secondary phases may have precipitated along with the hydration reaction of the original phases in the AOD slag [21]. The generation of hard soluble secondary phases results in a thicker solid layer, which inhibits chromium diffusion through the solid product layer. Therefore, the slopes of the chromium release fraction after 2 h were slightly smaller than those before 2 h, as shown in Fig. 3.

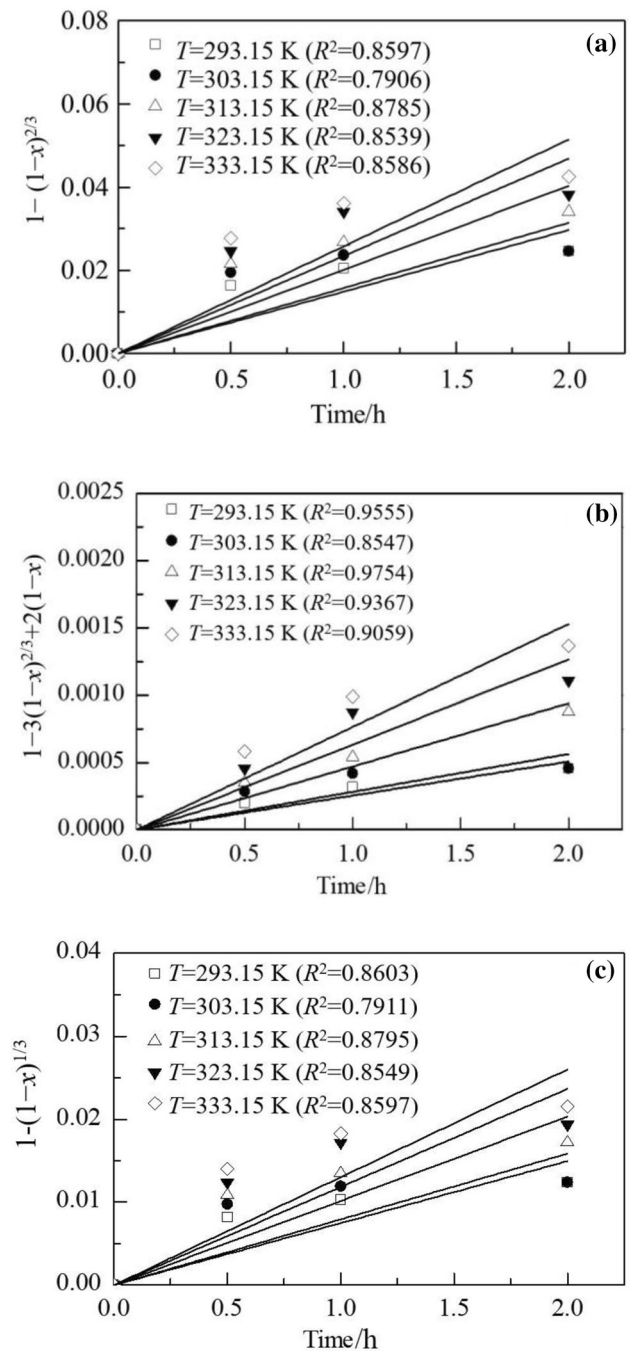


**Fig. 4** Kinetic models for quick leaching stage at different temperatures. **a** Equation (1) as a function of leaching time; **b** Eq. (5) as a function of leaching time; **c** Eq. (8) as a function of leaching time

In comparison with the quick leaching stage, the kinetics of chromium release during the slow leaching stage were more complicated. To confirm the kinetic model for the quick leaching stage and explore the kinetic control process of the slow leaching stage, the activation energy is calculated in the following section.

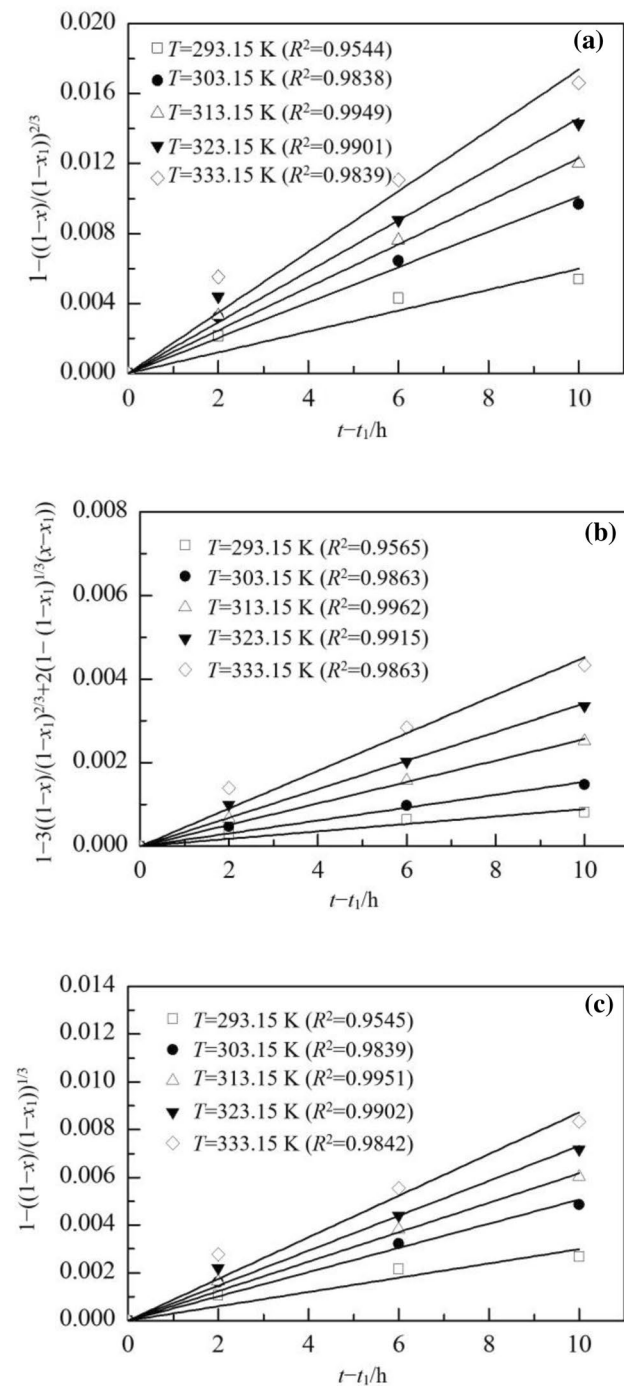


**Fig. 5** Kinetic models for slow leaching stage at different temperatures. **a** Equation (3) as a function of leaching time; **b** Eq. (6) as a function of leaching time; **c** Eq. (10) as a function of leaching time

### 3.4 Activation energy

During the actual leaching process, the kinetic steps for chromium release from AOD slag were more complicated than those described by the SCM. Therefore, the activation energy ( $E_a$ ) of chromium leaching was calculated based on

**Table 3** Relationship between  $E_a$  and velocity-determining step

Velocity-determining step	$E_a$ /(kJ mol <sup>-1</sup> )
Reaction control	> 42
Solid product diffusion control	< 13
Hybrid control <sup>a</sup>	13–42

<sup>a</sup>Both reaction control and solid product diffusion control

the chromium release fraction at different temperatures to evaluate the controlling processes during the quick and slow leaching stages. Table 3 shows the relationship between  $E_a$  and the velocity-determining step [22].

The temperature dependence of the reaction rate constant can be calculated by the Arrhenius equation as follows:

$$k = A \exp\left(\frac{-E_a}{RT}\right) \quad (12)$$

where  $A$  is the frequency factor; and  $R$  is the universal gas constant. This equation can be formulated as Eq. (13):

$$\ln k = \ln A - \frac{E_a}{R} \times \frac{1}{T} \quad (13)$$

The values of  $k$  at different temperatures, which correspond to the quick and slow leaching stages, can be calculated from the slope of the lines shown in Fig. 3. The Arrhenius plots ( $\ln k$  as a function of  $1/T$ ) for the quick and slow leaching stages are shown in Fig. 6. According to Eq. (13),  $E_a$  can be calculated based on the slope of the fitted lines in Fig. 6. During the quick leaching stage shown in Fig. 6a,  $E_a$  was 12.80 kJ/mol. This result suggests that solid product diffusion was the velocity-determining step due to being less than 13 kJ/mol. This result is also consistent with that obtained from the SCM. During the slow leaching stage shown in Fig. 6b,  $E_a$  was 20.92 kJ/mol. Therefore, hybrid control was the velocity-determining step because this value was in the range of 13–40 kJ/mol. This result further confirms the complexity of chromium release from the AOD slag during the slow leaching stage.

To elucidate the complexity of chromium release, a schematic representation of chromium release during the slow leaching stage is shown in Fig. 7. As shown in Fig. 7, spherical core 4 was assumed to be the unreactive chromium-bearing phase particle. Thin layer 3 was the multivariate phase, in which  $\text{Ca}_2\text{SiO}_4$  was the major component. Solid product layer 2 was the secondary phase that was gradually generated during the leaching process (i.e. hard soluble solid product). Liquid film 1 was the area with a concentration gradient close to the solid boundary. As previously mentioned, the dissolution reaction of the chromium-bearing phase did not occur at the surface of the chromium-bearing phase particle but occurred in thin layer 3. During the quick

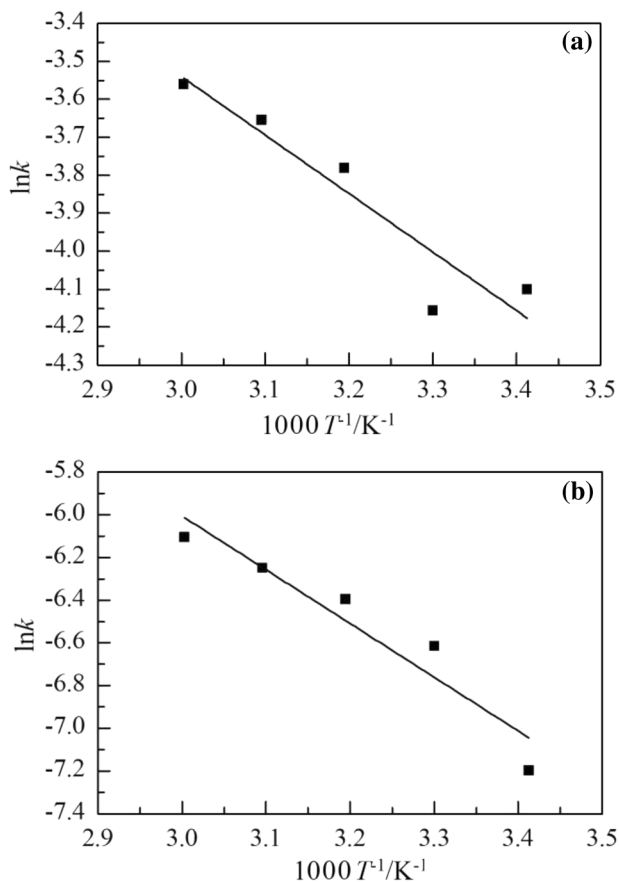


**Fig. 6** Arrhenius plots for chromium release from AOD slag. **a** Quick leaching stage; **b** slow leaching stage

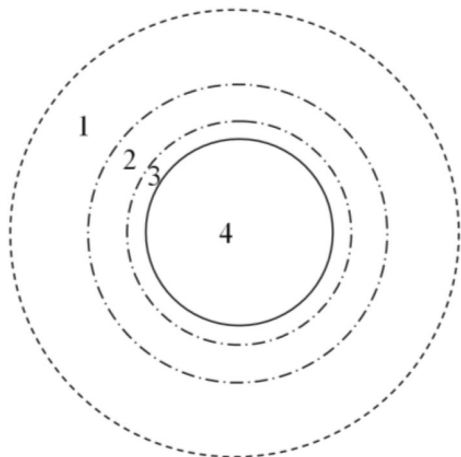


**Fig. 7** Schematic illustration of chromium release from AOD slag during slow leaching stage. 1—Liquid film; 2—solid product layer; 3—thin layer; 4—chromium-bearing phase particle

leaching stage, solid product layer 2 was almost not formed. The main solid product layer was thin multivariate-phase layer 3. Chromium could easily diffuse through the thin

layer, but the calculated  $E_a$  was 20.92 kJ/mol, which suggested hybrid control. During the slow leaching stage, this value was closer to 13 kJ/mol, which indicated that solid product diffusion predominantly controlled the chromium release. The hydration reaction of the original phases generated hard soluble secondary phases, which formed solid product layer 2 as the leaching time increased. The precipitation of the secondary phases thickened the solid product layer and decreased the release rate of chromium, which was consistent with the results shown in Fig. 3.

In the previous study [23], the activation energy for reaction control was higher than 40 kJ/mol, and the activation energy for physical adsorption/desorption was less than 40 kJ/mol, which indicated that physical adsorption/desorption influences chromium release from AOD slag during either the quick or slow leaching stage. Especially during the slow leaching stage, physical adsorption/desorption should have a significant impact on chromium release due to the thicker solid product layer. This conclusion corresponds to that reported in the study by Halim et al. [24]. The C–H–S gel ( $\text{CaH}_2\text{SiO}_4$ ) generated during the leaching process adsorbed chromium ions, which affected chromium release to a certain extent. Another study by Luo et al. [25] reported that the adsorption function of hydrated products (e.g. C–H–S gel) could solidify chromium ions and decrease their leaching value.

## 4 Conclusion

The release kinetics of chromium from AOD slag were explored based on HJ557-2009. The SCM was used to establish a kinetic model for chromium release from AOD slag. It was found that chromium release from the AOD slag occurred in two leaching stages (i.e. the quick and slow leaching stages) during the neutral leaching process. The chromium in AOD slag quickly released in the first 2 h but slowly released after 2 h. The chromium release fraction increased significantly as the temperature increased. Chromium release from the AOD slag was controlled by solid product diffusion during the quick leaching stage. A complicated process was involved during the slow leaching stage because the secondary phases could precipitate along with hydration reactions of the original phases in the AOD slag. The activation energy of the quick leaching stage was 12.80 kJ/mol, which suggested that solid product diffusion was the velocity-determining step. The activation energy for the slow leaching stage was 20.92 kJ/mol, which indicated that the chromium release was controlled by complicated hybrid control.

**Acknowledgements** This work was financially supported by the National Natural Science Foundation of China (Nos. 51704119 and

51574108), Natural Science Foundation of Hebei Province of China (No. E2017209243), Tangshan Municipal Project of Science and Technology (No. 19150201E) and School Funds for Distinguished Young Scientists (No. JQ201714).

## References

- [1] Z. Li, S. Zhao, X. Zhao, T. He, J. Hazard. Mater. 199–200 (2012) 448–452.
- [2] G. Adegoloye, A.L. Beaucour, S. Ortola, A. Noumowé, Constr. Build. Mater. 76 (2015) 313–321.
- [3] L. Kriskova, Y. Pontikes, Ö. Cizer, G. Mertens, W. Veulemans, D. Geysen, P. Tom Jones, L. Vandewalle, K. Van Balen, B. Blanpain, Cem. Concr. Res. 42 (2012) 778–788.
- [4] L. Kriskova, M. Erol, R.I. Iacobescu, S. Onisei, F. Vecchiocattivi, Y. Pontikes, J. Am. Ceram. Soc. 101 (2017) 1727–1736.
- [5] G. Adegoloye, A.L. Beaucour, S. Ortola, A. Noumowe, Constr. Build. Mater. 115 (2016) 171–178.
- [6] C.L. Zhen, G. Zhao, X.Z. Na, Y.H. Qi, J. Environ. Pollut. Prevent. 34 (2012) 76–79.
- [7] Q. Wang, P.Y. Yan, J.W. Feng, J. Hazard. Mater. 186 (2011) 1070–1075.
- [8] Y.M. Kuo, J.W. Wang, W.T. Wang, C.H. Tsai, J. Hazard. Mater. 186 (2008) 994–1001.
- [9] J. Li, B. Liu, Y. Zeng, Z.M. Wang, Z.Y. Gao, Environ. Monit. Assess. 189 (2017) 113.
- [10] J. Li, B. Liu, Y. Zeng, Z.M. Wang, Chemosphere 167 (2017) 360–366.
- [11] R.Y. Wang, R.H. Chen, L. Shi, Baosteel Tech. Res. 3 (2009) No. 4, 14–18.
- [12] Y. Samada, T. Miki, M. Hino, ISIJ Int. 51 (2011) 728–732.
- [13] B. Beverskog, I. Puigdomenech, Corros. Sci. 39 (1997) 43–57.
- [14] M. Kuhn, D. Mudersbach, in: Proceedings of the 2nd International Conference on Process Development in Iron and Steelmaking (SCANMET), Lulea, Sweden, 2004, pp. 369.
- [15] M. Aarabi-Karasgani, F. Rashchi, N. Mostoufi, E. Vahidi, Hydrometallurgy 102 (2010) 14–21.
- [16] E. Shirin, R. Fereshteh, S.K. Sadrezaad, Hydrometallurgy 82 (2006) 54–62.
- [17] Y.W. Chen, S. Tian, J. HLJ Environ. 32 (2008) 61–66.
- [18] L.Y. Bian, Environ. Sci. Manage. 32 (2007) 146–147.
- [19] E.A. Abdel-Aal, M.M. Rashad, Hydrometallurgy 74 (2004) 189–194.
- [20] O. Levenspiel, Chemical reaction engineering, 3rd ed., Wiley, New York, USA, 1999.
- [21] L.D. Windt, P. Chandler, J. Rose, Waste Manage. 31 (2011) 225–235.
- [22] S.K. Sadrezaad, Kinetic processes in materials engineering and metallurgy, 2nd ed., Amirkabir Publications Organization, Tehran, Iran, 2004.
- [23] F. Habashi, Principles of extractive metallurgy, Gordon and Breach, New York, USA, 1980.
- [24] C.E. Halim, S.A. Short, J.A. Scott, R. Amal, G. Low, J. Hazard. Mater. 125 (2005) 45–61.
- [25] Z.Q. Luo, S.X. Zhang, Y.L. Shi, Bull. Chin. Ceram. Soc. 32 (2013) 1206–1211.